Water Science & Technology

IWA PUBLISHING

Water Science & Technology Vol 89 No 8, 2020 doi: 10.2166/wst.2024.109

Enhanced properties of a positive-charged nanofiltration membrane containing quaternarized chitosan through second interfacial polymerization for the removal of salts and pharmaceuticals

Xinhui Bai[a,†], Yuting Lu[b,†], Mudan Wang[a], Xinyang Yu[a] and Zhonghua Huang[a,*]

[a] Key Laboratory of New Membrane Materials, Ministry of Industry and Information Technology, School of Environmental and Biological Engineering, Nanjing University of Science and Technology, Nanjing 210094, China
[b] School of Sino-French Engineer, Nanjing University of Science and Technology, Nanjing 210094, China
*Corresponding author. E-mail: hzhlqfox@njust.edu.cn
†X.B. and Y.L. contributed equally to this manuscript.

ABSTRACT

Nanofiltration (NF) membrane technology has been widely used in the removal of salts and trace organic pollutants, such as pharmaceuticals and personal care products (PPCPs), due to its superiority. A positive-charged composite NF membrane with an active skin layer was prepared by polyethyleneimine (PEI), trimethyl benzene chloride, and quaternate chitosan (HTCC) through second interfacial polymerization on the polyethersulfone ultrafiltration membrane. The physicochemical properties of the nanocomposite membrane were investigated using surface morphology, hydrophilicity, surface charge, and molecular weight cut-off (MWCO). The influence of the concentration and reaction time of PEI and HTCC was documented. The optimized membrane had a MWCO of about 481 Da and possessed a pure water permeability of 25.37 $L{\cdot}m^{-2}{\cdot}h^{-1}{\cdot}MPa^{-1}$. The results also exhibited salt rejection ability as $MgCl_2 > CaCl_2 > MgSO_4 > Na_2SO_4 > NaCl > KCl$, showing a positive charge on the fabricated membrane. In addition, the membrane had higher rejection to atenolol, carbamazepine, amlodipine, and ibuprofen at 89.46, 86.02, 90.12, and 77.21%, respectively. Moreover, the anti-fouling performance and stability of the NF membrane were also improved.

Key words: interfacial polymerization, NF membrane, PPCPs, separation performance

HIGHLIGHTS

- A positive-charged nanofiltration (NF) membrane was modified by quaternate chitosan (HTCC) via second interfacial polymerization.
- HTCC, containing quaternarized chitosan, was prepared with natural chitosan.
- Anti-fouling performance and stability were improved.
- The NF membrane surface was positively charged.
- Salts and trace organic pollutants, such as pharmaceuticals and personal care products, were removed.

GRAPHICAL ABSTRACT

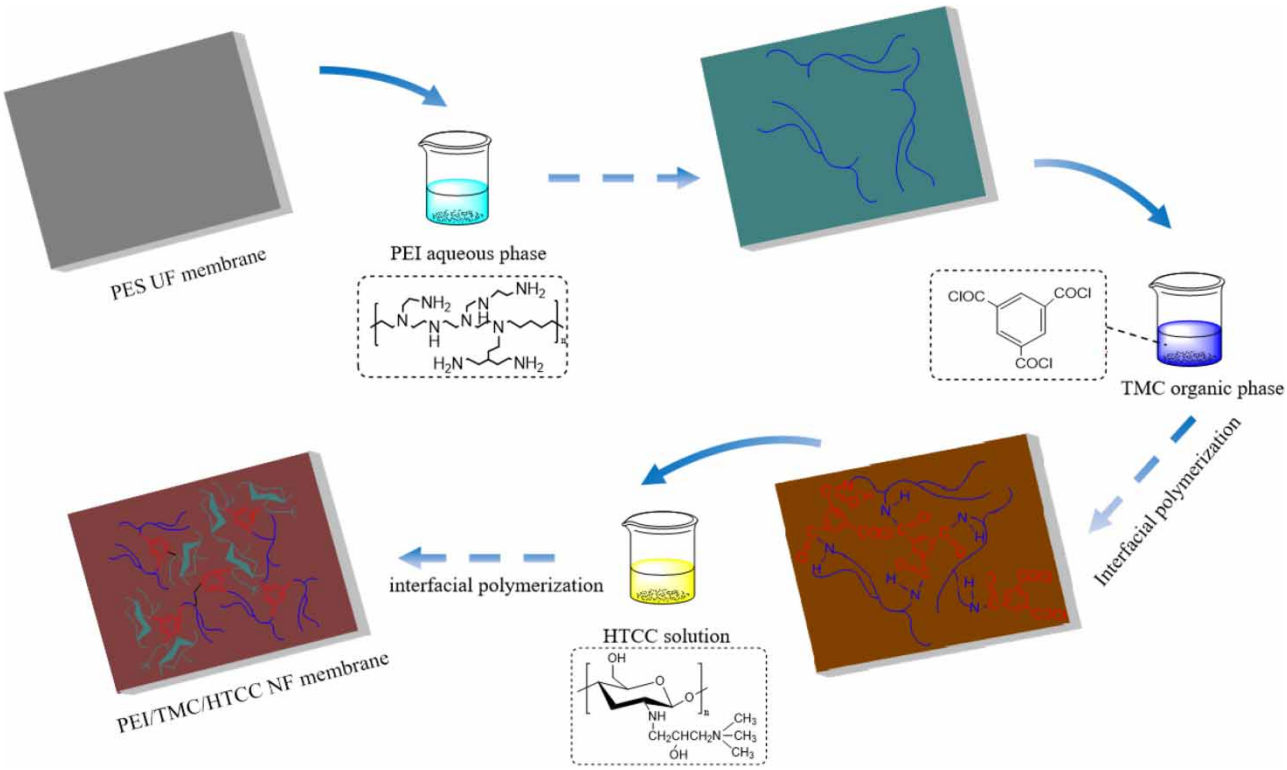

1. INTRODUCTION

Nowadays, pharmaceuticals and personal care products (PPCPs), which are bioactive trace pollutants in different environmental compartments, such as surface water, drinking water, groundwater, and sediments, are progressive issues due to the increasing urbanization (Ellis 2006; Liu *et al.* 2023). As PPCPs are abundant in the environment and possess significant ecological risks (endocrine disruption, bioaccumulation, inducement of bacterial antibiotic resistance, clinical toxicity, etc.), dealing with PPCPs effectively has become a serious problem (Liu *et al.* 2020; Oluwole *et al.* 2020). The major route for pharmaceutical residues to reach the aquatic environment is the direct emissions of drugs, and another source is most probably excretion from patients undergoing pharma treatments (Montforts 2006; Fatta-Kassinos *et al.* 2011). Kosma *et al.* (2010) investigated the residues of 11 PPCPs in the municipal and hospital wastewater treatment plants of Ioannina City in Western Greece. The results showed the occurrence of all target compounds in the wastewater samples and the achievement of the highest removal rate during biological treatment, which were satisfactory except for diclofenac and carbamazepine (CBZ). These could produce reproductive, neurological, and other toxicological or carcinogenicity effects on humans and other organisms through drinking water and food chains (Dai *et al.* 2014; Kosma *et al.* 2014). Besides, on account of the slight PPCP concentration and their intricate chemical structure, technologies used frequently in sewage treatment plants might not be efficient enough to remove them. So, it is imminent to find other especially impactful approaches to remove PPCPs. Owing to higher permeate flux and less rejection of monovalent salts, nanofiltration (NF) membranes exhibit more advantages in preventing PPCPs from entering aquatic environments (Bellona & Drewes 2007; Radjenović *et al.* 2008; Zhao *et al.* 2017; Liu *et al.* 2018a).

NF membranes have a pore size typically of 1 nm with properties in between the ultrafiltration (UF) membrane and the reverse osmosis (RO) membrane, which are all pressure-driven separation processes (Oatley-Radcliffe *et al.* 2017). Due to the moderate operating pressure and a high retention rate of small molecules, NF membranes have been widely utilized in desalination, wastewater treatment, and liquid concentration (Guo *et al.* 2021). Currently, NF membranes have attracted considerable attention for improving PPCP removal for water reclamation (Lin *et al.* 2018). Košutić *et al.* (2007) investigated the removal of antibiotics by RO/NF from model wastewater of a manufacturing plant producing veterinary

pharmaceuticals. The rejection of the examined antibiotics by the selected RO and the tight NF membranes was acceptably high. The dominant rejection mechanism of the examined ionizable antibiotics by all the membranes was the size exclusion effect. Mansourpanah *et al.* (2011) applied trimesoyl chloride (TMC) and piperazine as reagents for the preparation of poly(piperazine amide) on a polyethersulfone UF support. The rejection of tetracycline antibiotics and sulfonamides by the NF/RO membrane exceeded 90%. Donnan exclusion and mobility of the ions across the membrane are two important factors affecting the rejection capability of ions for charged membranes. Therefore, the rejection mechanisms of trace organic micropollutants by NF membranes mainly include steric hindrance and electrostatic repulsion (Semião & Schäfer 2013; Semião *et al.* 2013). Typical NF membranes with thin film composite (TFC) structures have been fabricated by the interfacial polymerization (IP) of the diamine and acyl chloride (Shen *et al.* 2019). Lin *et al.* modified NF90 with 3-sulfopropyl methacrylate potassium salt and 2-hydroxyethyl methacrylate applying for the removal of CBZ, ibuprofen (IBU), sulfadiazine, sulfamethoxazole, sulfamethazine, and triclosan (Lin *et al.* 2019).

Nowadays, IP is one of the most common methods to develop composite NF membranes, which consist of a dense polyamide functional barrier layer and a porous support membrane (Bi *et al.* 2018; Chiao *et al.* 2020). They can both dominantly influence the NF performance including the water flux and salt rejection (Zhang *et al.* 2004). Compared to other techniques, the method of IP has several advantages such as easy purification of products, reproducible results, and good polymerization yield. Furthermore, IP is also applied to produce high-quality polyaniline nanofibers with control over their size, morphology, and nanofiber diameter (Li *et al.* 2015). Tang *et al.* 2008 fabricated a novel positive-charged NF hollow fiber membrane for lithium and magnesium separation through the IP of decentralized application and TMC on the polyacrylonitrile support membrane. The research demonstrated the effects of the reaction time of polymerization and the concentration of reactive monomers on the performance of the composite membrane. The permeability of a single salt followed $LiCl > NaCl > MgSO_4 > MgCl_2$ at $pH = 9.5$ and the negative repulsion of Li^+ ions was found in the mixed solution of LiCl and $MgCl_2$. Tsuru *et al.* 2013 employed triethanolamine and TMC via IP to fabricate the polyester Kenner membrane with good acid resistance, which studied the effects of polymerization time, monomer concentration, and pH value of the aqueous solution. The tertiary amine groups of the film surface layer becoming quaternary ammonium groups contribute to advancing the flux of the membrane at low pH. In the research of Tsuru *et al.* (Wang *et al.* 2002), the permeability of the obtained NF membrane greatly increased through two-step IPs using isophthaloyl chloride and trimesoyl chloride. Recently, many efforts have been made to improve the separation performance by introducing polyethyleneimine (PEI) into the aqueous phase during the IP process.

PEI, as a cationic polyelectrolyte, contains abundant amine groups and the proportion of primary amine, secondary amine, and tertiary amine is 1:2:1, which has been widely verified for preparing high positively charged and excellent hydrophilic TFC NF membranes via the IP process thanks to its high charged density, easy protonation, and easy preparation (Lee *et al.* 2004; Xu *et al.* 2015; Shen *et al.* 2020; Bridge *et al.* 2022). Tao *et al.* 2022 developed a composite NF membrane-grafted PEI on the polyamide layer, in which the removal rate for heavy metals reached 90% and the water flux reached 74 $L{\cdot}m^{-2}{\cdot}h^{-1}{\cdot}MPa^{-1}$. Xu *et al.* (2019a) designed a double quaternary ammonium salt to modify the PEI polyamide NF membrane. The permeability of the modified PEI membrane was 212 $L{\cdot}m^{-2}{\cdot}h^{-1}{\cdot}MPa^{-1}$ and was 4.4 times that of the original PEI film. At the same time, the $MgCl_2$ retention rate remained at 95%. El-Gendi *et al.* 2018 fabricated a positively charged NF membrane with abundant $-NH_3^+$ and $-NH_2^+$ groups for the separation of Mg^{2+} and Li^+ from salt lake brine, which had a high Mg^{2+}/Li^+ mass ratio. The NF membrane was prepared by IP between PEI and TMC on the support of polyethersulfone (PES) UF membrane, and the salt rejection followed the order: $MgCl_2$ (94.8%) > $MgSO_4$ (84.1%) > Na_2SO_4 (81.4%) > NaCl (36.9%) > LiCl (30.6%). Huang *et al.* 2015 produced new PEI asymmetric membranes to get selective polymeric membranes with high flux fitting for the separation of organic molecules from aqueous mixtures by NF.

Herein, we aimed to construct a positively charged NF membrane with comprehensive rejection to PPCPs of different physicochemical properties using a new positively charged compound quaternate chitosan (HTCC) by nucleophilic substitution reaction with glycidyl trimethyl ammonium chloride (GTMAC), PEI, and TMC via second IP (SIP). The original loose PES membrane was capable of immobilizing the positively charged polyamide layer formed by IP of PEI, TMC, and HTCC. The multilayer morphology, hydrophilicity, and surface charge were analyzed by SEM, atomic force microscope (AFM), water contact angle, and zeta potential, respectively. Meanwhile, we investigated the concentration and soaking time of PEI and HTCC on the membrane performance, respectively. In addition, the water permeability and separation capability of diluted salts and PPCPs of the modified membrane were evaluated.

2. EXPERIMENTAL

2.1. Materials

Chitosan (CTS, weight-averaged molecular weight Mw ≈ 150 kDa, Sinopharm Chemical Reagent Co., Ltd) was dissolved in the solvent acetic acid ($CH_3COOH \geq 99.5\%$, Sinopharm Chemical Reagent Co., Ltd). The PES UF membrane (MWCO = 10 kDa) was provided by Ande Membrane Separation Technology Engineering Co., Ltd (Beijing, China). Polyethyleneimine was obtained from Maclean Biotechnology Co., Ltd. (Shanghai, China). GTMAC with a purity of ≥95% was purchased from Shanghai DB Biotechnology Co., Ltd (China). Polyethylene glycol with molecular weights of 400, 600, 800, 1,000, and 1,500 g/mol purchased from Chengdu Kelong Chemical Reagent Co., Ltd was used as the model neutral solutes to estimate the MWCO of the obtained membrane. Trimethylbenzene chloride was provided by Saan Chemical Technology Co., Ltd (Shanghai, China). Hexane was provided by Titan Technology Co., Ltd (Shanghai, China). Atenolol (ATE), CBZ, amlodipine (AML) and IBU were kindly provided by the China Institute of Food and Drug Control City, China. Other chemicals, including inorganic salts, ethanol, and sodium hydroxide, were procured from Sinopharm Chemical Reagent Co., Ltd (China). All aqueous solutions were prepared using purified water with a resistance of 18.2 MΩ·cm.

2.2. Synthesis of HTCC

The specific preparation method of HTCC was previously described in published literature (Afonso *et al.* 2001). Two grams of CTS powder was dissolved in 100 mL of acetic acid with a concentration of 2 wt%. Then, a 10 wt% NaOH solution was added to adjust the pH to 10 and to precipitate the CTS. The reaction proceeded under stirring for 4 h to allow the CTS to be fully alkalized. Then, the solution was centrifuged under 3,000 r/min and turned into a flask containing 30 mL isopropanol as medium with continuously stirring for 3 h at 70 °C. Then, a certain number of mole GTMAC (n_{CTS}:n_{GTMAC} = 1:4) was added to the solution at 80 °C for 8 h. After cooling, the reaction solution was washed thrice with a 250 mL acetone solution. The precipitated solids were put into the oven at 80 °C until fully dried. Finally, the obtained material was ground into powder.

2.3. Membrane fabrication

The fabrication process of a composite membrane is shown in Figure 1. First of all, a proper amount of fine HTCC powder was added to the solution containing a certain concentration of NaCl, which was used as support salts under agitation. Meanwhile, the circular pieces of PES membranes with an area of 12.56 cm^2 were prewetted by deionized water for 1 h and then immersed in a mixed aqueous solution of 1.5% PEI, 0.1% SDS, and 0.1% Na_2CO_3 for 20 min. The membrane was immersed in an *n*-hexane solution having a mass concentration of 0.2% TMC for 5 min after the excess PEI mixture on the membrane was removed by a rubber roller. This process created a PEI/TMC composite membrane. Secondly, after the excess *n*-hexane solution was evaporated, the membrane was immediately immersed in the prepared HTCC casting solution for 15 min for further modification and then dried in an oven at the temperature of 50 °C until drying. Finally, the PEI/TMC/HTCC composite NF membrane was prepared through SIP.

2.4. Membrane characterization

The chemical structure of the membrane surface was observed by the Fourier transform infrared spectrometer (FTIR/ATR Nicolt iS5). The sample with 1 cm^2 was placed on the loading stage, and then the detection device was pressed on the center of the sample module to detect, to get the FTIR spectrum in the range of 3,500–500 cm^{-1}. A scanning electron microscope (JEOLJSM-6380LV) was used to scan the surface and cross-section micromorphology of the PES substrate and the modified membrane. The morphologies of membranes were observed under appropriate magnifications of 5 and 100 k. The sample, needed to be dehydrated and golded before the surface morphology, was observed. An AFM (Dimension 310) was utilized to observe the surface structure and roughness of the modified membrane. The static contact angle was employed by a DSA30 contact angle system to discuss the change in its hydrophilicity. Additionally, the streaming potential method was adopted to detect charging Zeta potential on the surface of a dually charged membrane using the electrokinetic analyzer (SurPASS™ 3, Austria) with 1 mM KCl solution as an electrolyte solution, to determine the isoelectric point on the surface of the membrane and analyze the influence of external pH on the surface charge.

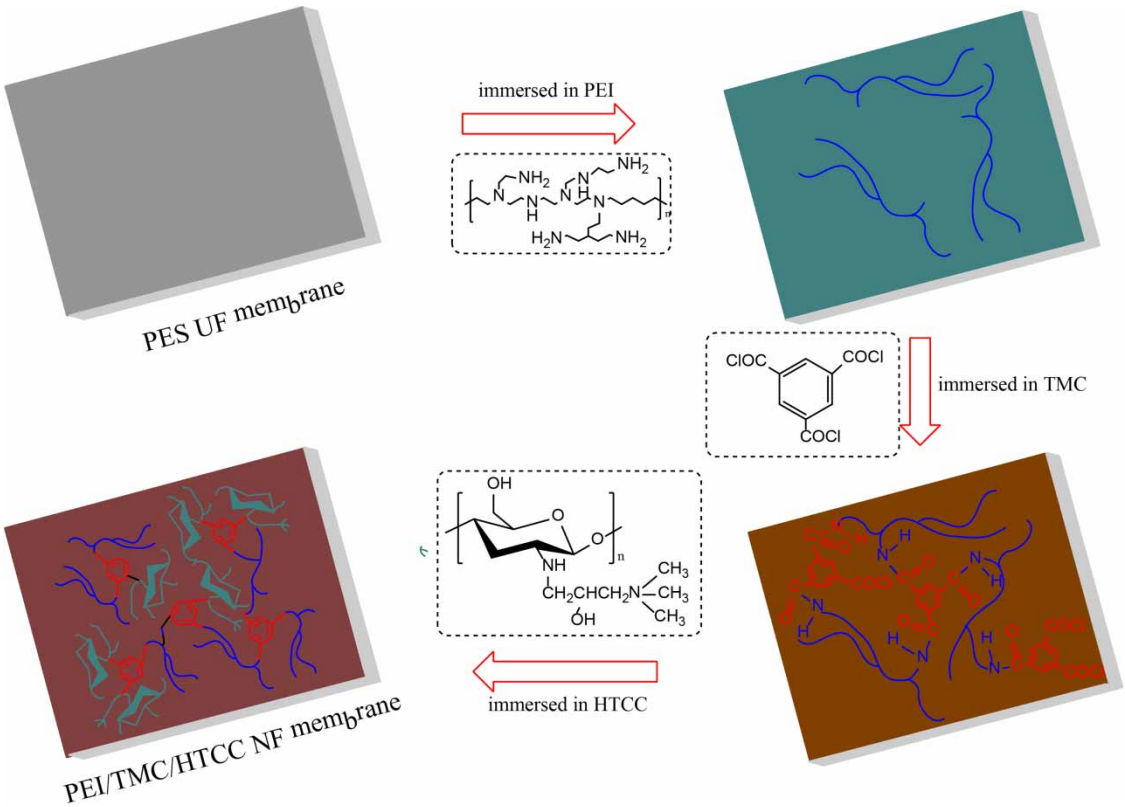

Figure 1 | Preparation scheme of the PEI/TMC/HTCC composite membrane.

2.5. Evaluation of membrane performance

The permeability coefficient of pure water was estimated by the following Spiegler–Kedem equation:

$$J_V = L_P(\Delta P - \sigma \Delta \pi) \tag{1}$$

where J_V is the solvent permeation rate, L_P is the permeability coefficient, ΔP is the pressure, σ, and $\Delta\pi$ are reflection coefficient and osmotic pressure, respectively. In this experiment, there were no residual ions due to pure water and $\sigma\Delta\pi$ is approximately 0, so the theoretical model of Spiegler–Kedem could be simplified as $J_V = L_P \cdot \Delta P$.

The MWCO of the modified membrane was measured by rejection experiments of neutral organic solutes (1 g/L) with molecular weights ranging from 100 to 1,000 Da at 6 bar. The concentration of organic matter in the material liquid and the osmotic liquid was detected by the total organic carbon analyzer. According to the literature, it was known that the molecular weight with 90% retention was defined as MWCO (Liu *et al.* 2018b).

The separation performance of the developed NF membrane was evaluated by a laboratory-scaled cross-flow device. The effective area for each NF membrane was 12.56 cm^2. The samples were preoperated at 6 bar for 30 min to reach a stable state. The rejection of inorganic salt solutions, such as $MgCl_2$, $CaCl_2$, $MgSO_4$, Na_2SO_4, NaCl (0.5 g/L), and PPCPs (0.5 g/L), ran at 5 bar with a cross-flow velocity of 40 mL/min. The average value of three measurement data was defined as the final value for each sample. The permeation flux (Q, L/m^2·h) and rejection (R, %) were calculated by the following equation:

$$Q = \frac{V}{At} \tag{2}$$

where V, A, and t represent the volume of permeated water, effective membrane area, and permeation time, respectively.

$$R = \left(1 - \frac{C_P}{C_f}\right) \times 100\% \tag{3}$$

where C_f and C_P are the solute concentrations in feed and permeate, respectively. The concentration of salt solution before and after interception was obtained by an electrical conductivity meter (METTLER TOLEDO, JB/T9366, China). The concentrations of different PPCPs were determined using high-performance liquid chromatography (Agilent, 1260 infinity, USA).

To estimate the anti-fouling property of the membranes, the flux recovery of two NF membranes during several cycles of permeating the sodium alginate solution at a concentration of 0.5 g/L was tested. To complete the cycle, the flow rate of pure water was measured and recorded as J_0 (L m^{-2} h^{-1}). The sodium alginate solution was then permeated through the membrane and the flux was measured as J_P. After 30 min of hydraulic washing, the pure water flux was re-measured and recorded as J_t. The evaluating parameters of the total flux decline ratio (DR_t) and the flux recovery ratio (FRR) were calculated by the following equations:

$$DR_t = \frac{J_0 - J_P}{J_0} \tag{4}$$

$$FRR = \frac{J_t}{J_0} \times 100\% \tag{5}$$

where J_0, J_P, and J_t are the initial flux, membrane recovery flux, and the flux of the membrane after being contaminated by organic matter, respectively.

3. RESULTS AND DISCUSSION

3.1. Influence factors on the performance of membrane separation

Firstly, the effect of fabrication conditions on the separation performance of the PEI/TMC/HTCC NF membranes was investigated to achieve both high flux and salt rejection. The concentration of the aqueous monomer and its loading on the membrane directly affects the rate of IP and the nature of the polymerization product, so it is significant to find a suitable PEI monomer concentration and soaking time. As illustrated in Figure 2(a) and 2(b), the flux and the rejection of Na_2SO_4 and $MgCl_2$ (0.5 g/L) under 6 bar of the resultant membranes were studied. When the concentration of PEI and soaking time increased, the rejection of Na_2SO_4 and $MgCl_2$ increased, but the flux decreased. More PEI was attached to the membrane surface, which increased the degree of cross-linking and the density of the network structure (Zhang *et al.* 2014). However, when the concentration of PEI was too high or the soaking time was too long, the IP rate increased sharply causing the polyamide functional layer to thicken rapidly (Zhang *et al.* 2016). The complete network-like macromolecule was difficult to form in a limited time, which resulted in more wrinkles and more defects on the membrane surface. Therefore, in this study, the 1.5% PEI concentration and 20 min PEI soaking time were employed.

As shown in Figure 2(c), the rejection for $MgCl_2$ increased to 92% ascribed to the electrostatic effect when the HTCC concentration was 0.5%, so 0.5% was the best concentration of HTCC. This was due to the reaction of acid chloride groups that were left on the PEI/TMC membrane with HTCC, and the introduction of quaternary ammonium groups in the HTCC directly modified the surface electrical properties of the membrane from negative to positive, so that the rejection of $MgCl_2$ was higher than that of Na_2SO_4 (Xiang *et al.* 2022). As the concentration of HTCC increased, the density of HTCC molecules near the outer surface of the polyamide layer increased, and the consumed acid chloride groups also increased forming a tighter membrane surface structure, which showed a certain degree of increase in rejection and decline in flux. When the concentration of HTCC exceeded 0.5%, the rejection of Na_2SO_4 was significantly reduced due to the increase of the positive charge on the surface of the membrane and the rejection of $MgCl_2$ was only slightly increased. At the same time, the viscosity of the HTCC solution was too large to block the pores of the membrane, resulting in a continuous decrease in flux.

As exhibited in Figure 2(d), when the soaking time reached 10 min, the $MgCl_2$ rejection rate was higher than the rejection rate of Na_2SO_4 and the rejection of the two salts tended to be stable when the reaction time between 15 and 30 min, indicating that the residual acid chloride groups had been largely consumed when the reaction time was 15 min. When the reaction

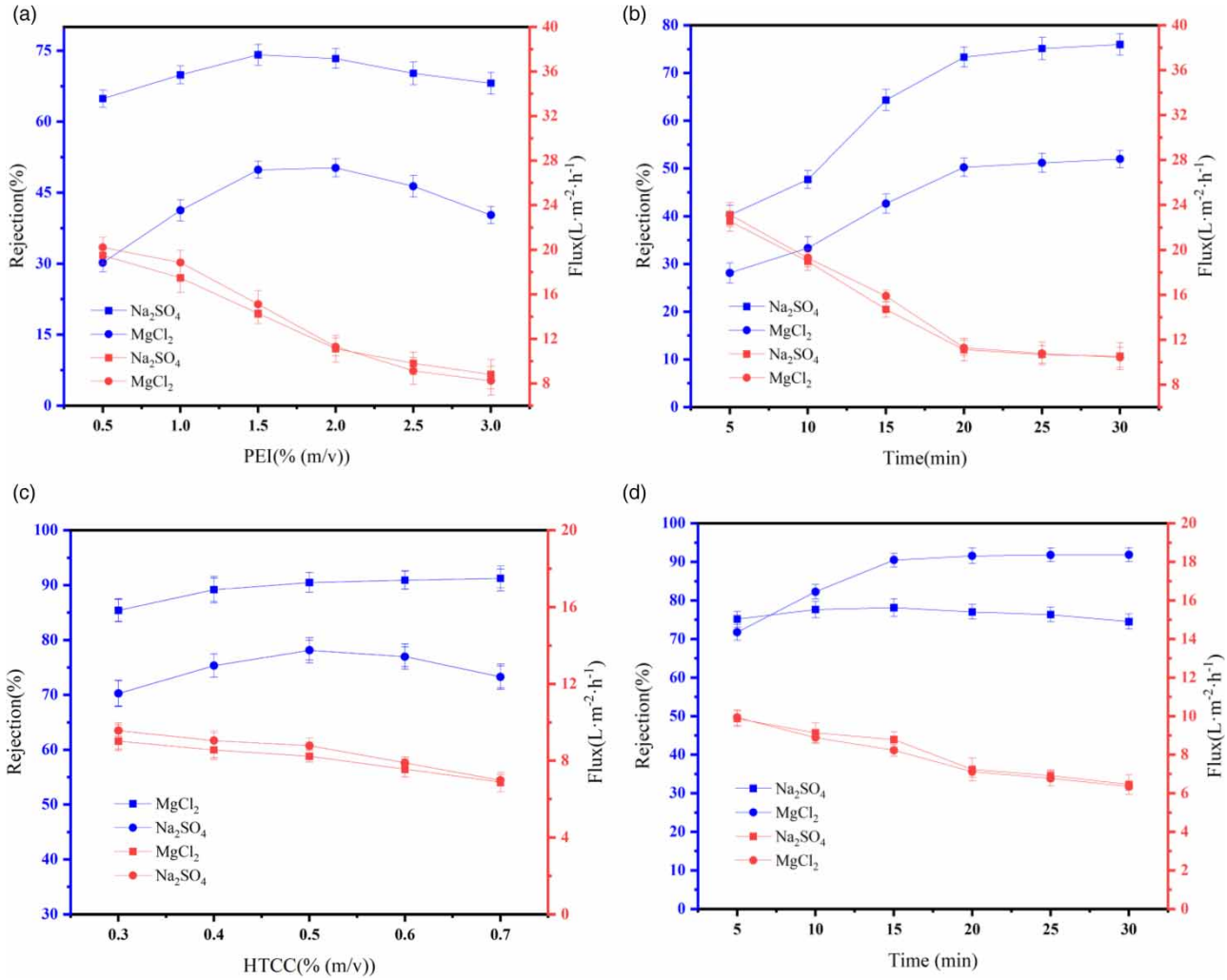

Figure 2 | Influence of PEI concentration (a), PEI soaking time (b), HTCC concentration (c), and HTCC soaking time (d) on the salt rejection and flux by the PEI/TMC/HTCC membrane.

time exceeded 15 min, the rejection of Na_2SO_4 decreased slightly while the rejection of $MgCl_2$ a little increased, and the flux continued to decrease. This was because a small amount of HTCC molecules were still diffusing toward the interface and gathered on the surface of the membrane with a positive charge and high viscosity resulting in the pores of the membrane being blocked. Taken together, the reaction time was 15 min for the optimal condition.

3.2. Surface morphologies and chemical composition

Figure 3(a1)–3(c1) reveals the surface morphologies of the PES membrane, the PEI/TMC membrane, and the PEI/TMC/HTCC membrane under 10 and 100k magnification. It can be seen in Figure 3(a1) that small holes were obviously visible on the membrane surface. Compared to the PES membrane, the obvious wrinkled structure was observed on the top surface of the PEI/TMC membrane and the PEI/TMC/HTCC membrane. The overall shape of the polymer could be exhibited in the figure of the upper right corner of Figure 3(b1) and 3(c1), showing obvious leaf polymer adheres, which was the characteristic form of polyamide. These changes made the surface structure of the PEI/TMC membrane and the PEI/TMC/HTCC membrane more compact and more stable than the PES membrane. Figure 3(a2)–3(c2) shows the cross-sectional morphology of the PES membrane, the PEI/TMC membrane, and the PEI/TMC/HTCC membrane at 1 and 5k magnification. Compared with the PES membrane, the average skin-layer thickness of the PEI/TMC membrane approximately increased from 0.84 to 1.23 μm. The reason was that IP reduced the pore size and increased the discontinuity of the PEI/TMC membrane. Moreover,

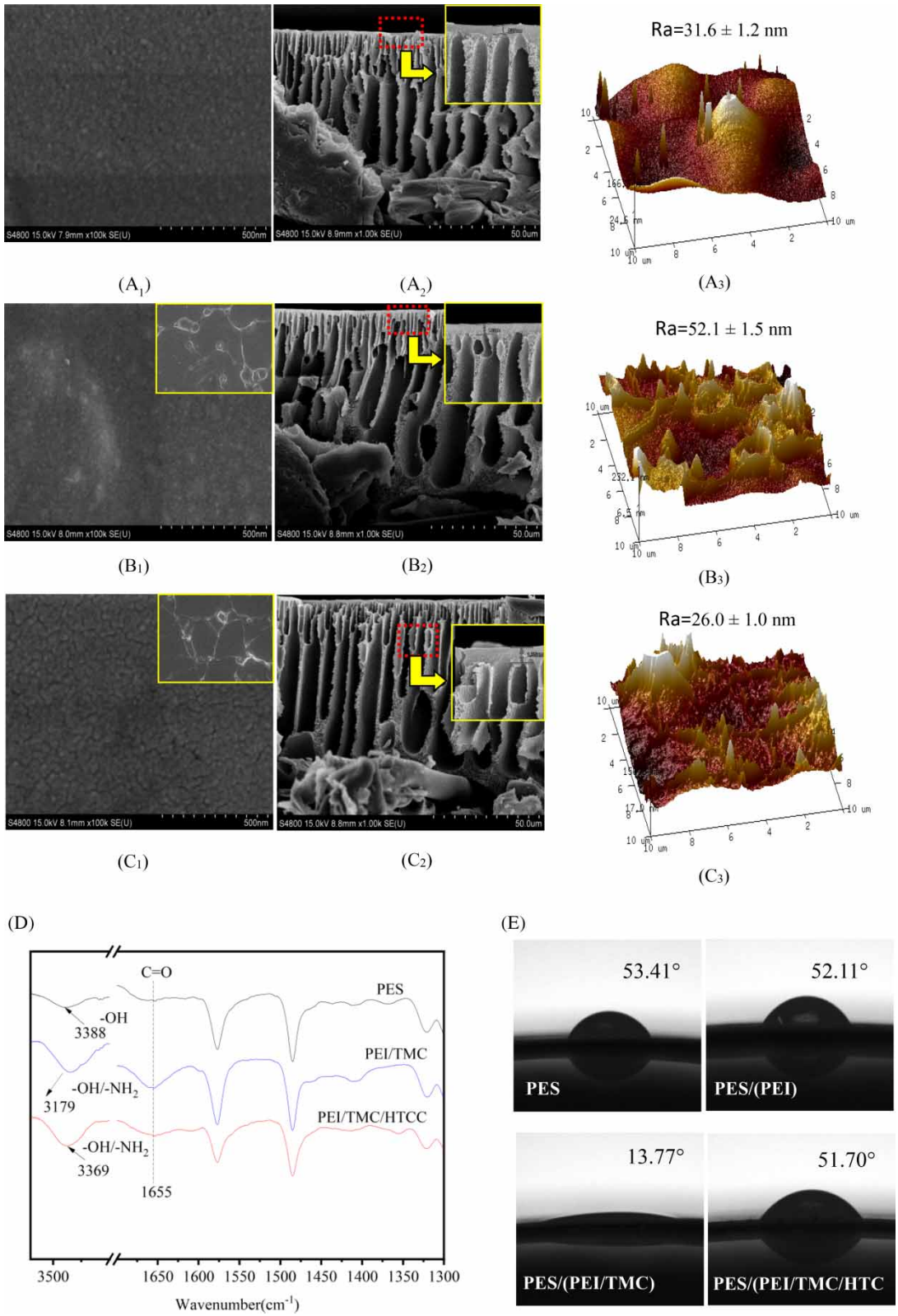

Figure 3 | Scanning Electron Microscope images: (1) top view, (2) cross-section view, and (3) AFM 3D images of the PES membrane (A), the PES/(PEI/TMC) membrane (B), the PES/(PEI/TMC/HTCC) membrane (C), FTIR spectrum (D), and contact angle (E) of membranes.

the average thickness of the PEI/TMC/HTCC membrane increased approximately from 1.23 to 1.35 μm compared with the PEI/TMC membrane, proving that HTCC was introduced into the surface of the PEI/TMC membrane. This implies that the SIP's average thickness was about 0.12 μm.

The characteristic AFM 3D images and the average roughness of different membrane samples are shown in Figure 3(a3)–3(c3). It could be seen that M0 had an obvious ridge-and-valley structure with an averaged RMS roughness of 31.6 nm. After IP of PEI and TMC on the PES membrane, it could be observed that the surface roughness of the modified membrane had been increased relatively with more ridge-and-valley structure, attributing to the formation of the cross-linked network structure of the selective layer by PEI (Kong *et al.* 2016). In addition, the RMS value of the PEI/TMC membrane increased to 52.1 nm, which proves that PEI and TMC strongly reacted, forming polyamide attached to the surface of the PES membrane, causing a sharp increase in roughness. Compared with the PEI/TMC membrane, the surface roughness of the PEI/TMC/HTCC membrane was significantly increased to 26.0 nm owing to a relatively slow reaction process between HTCC and the remaining TMC, encapsulating the polyamide layer of the PEI/TMC membrane.

As shown in Figure 3(d), the PES membrane illustrated a normal water peak at 3,388 cm^{-1}, while the PEI/TMC membrane showed a significant increase in the absorption peak volume at 3,179 cm^{-1} and a redshift. On the one hand, this was due to –COCl which originated from incompletely reacted TMC. It underwent hydrolysis to form –COOH, resulting in an increase in the absorption peak area. On the other hand, PEI and TMC were polymerized to form –CONH–, and the –OH peak overlapped with the –NH peak, causing the absorption peak to redshift (Ouyang *et al.* 2019). The absorption peak of the PEI/TMC/HTCC membrane at 3,179 cm^{-1} showed a blueshift to 3,369 cm^{-1}, which is ascribed to the introduction of –OH by the load of HTCC. The PEI/TMC composite NF membrane exhibited a typical absorption peak of C = O on $-CONH_2$ at 1,655 cm^{-1} (C = O stretching, amide I), which indicated IP (Semião & Schäfer 2013). The absorption peak at 1,655 cm^{-1} on the PEI/TMC/HTCC membrane was smaller because the composite structure introduced by the second step had no amide bond production and covered the original amide structure.

The visual diagram of the contact angle of the PES membrane, PES/(PEI), PES/(PEI/TMC), and PES/(PEI/TMC/HTCC) membrane is shown in Figure 3(e). By introducing a layer of PEI, the water contact angle of the PES/(PEI) membrane was a little smaller than that of the PES membrane, illustrating that the amino group in PEI improved the hydrophilicity of the PES membrane. When the interface polymerization between PEI and TMC occurred, the contact angle of the PEI/TMC membrane dropped to 13.77° because the acid chloride group on the remaining TMC was hydrolyzed to form excellent hydrophilic carboxyl groups (Li *et al.* 2022). After SIP, the contact angle of the PES/(PEI/TMC/HTCC) membrane quickly rose to 51.70°, thanks to the massive consumption of –NH on the HTCC and the reduction of hydrolysis of acid chloride groups.

3.3. MWCO and water permeability coefficient of pure water

As illustrated in Figure 4(a), with the increase of the operation pressure, the pure water flux of the composite membrane increased, which presented a linear relationship. According to Formula 1, the pure water permeability coefficient of the

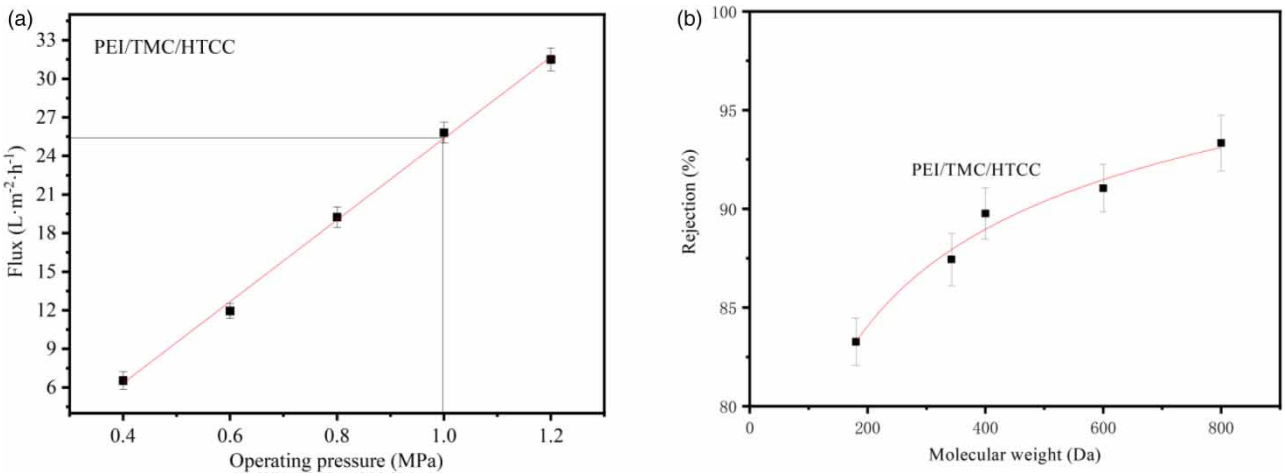

Figure 4 | Permeability coefficient of pure water (a) and molecular weight cut-off (b) of the PEI/TMC/HTCC membrane.

composite membrane was 25.37 $L \cdot m^{-2} \cdot h^{-1} \cdot MPa^{-1}$. At present, the recognized interception mechanism includes Donnan exclusion, dielectric effects, and steric hindrance. To discuss the MWCO of the NF membrane, the modified membrane was detected by the retention of a series of neutral organic solutes. As shown in Figure 4(b), the molecular weight was 481 Da when the removal rate of neutral organic compounds reached 90%, which belonged to the category of molecular weight (200–1,000 Da) of the NF membrane. The function obtained by fitting is $y = 225 \times {}^{0.03} - 174$, $R^2 = 0.9560$. In addition, the retention curve was steeper, which indicated high quality for the composite NF membrane and good separation of solutes with different molecular weights.

3.4. Separation performance

3.4.1. Rejection of diluted salts

The removal of single salts (0.5 g/L) was determined to evaluate the separation performance of the modified membrane under 6 bar. The experimental results are presented in Figure 5(a). The rejection of the PEI/TMC/HTCC membrane to different single salts followed the order of $MgCl_2 > CaCl_2 > MgSO_4 > Na_2SO_4 > NaCl > KCl$, which had high retention for high-valent cations (Mg^{2+}, Ca^{2+}, etc.), indicating that the electrostatic effect of the composite membrane on the cation was stronger, and the positive chargability of the membrane surface was reflected. The change curve of the PEI/TMC/HTCC membrane surface potential with pH in Figure 5(b) coincided with this result. After the polyelectrolyte IP, the overall positive charge of the PEI/TMC/HTCC membrane was greatly improved because the cortex of the functional layer contained unreacted primary, secondary, and tertiary amines that were positively charged under acidic and neutral conditions. On the contrary, the interception order of six inorganic salt solutions of the PEI/TMC membrane without modification by HTCC was $Na_2SO_4 > MgSO_4 > MgCl_2 > CaCl_2 > NaCl > KCl$, which was consistent with the interception law of negatively charged NF membrane and the change curve of the PEI/TMC membrane surface potential with pH in Figure 5(b) (Gu *et al.* 2020). Table 1 summarizes the performance of NF membranes reported in the recent literature. Compared to the previously reported membrane, the lab-fabricated PEI/TMC/HTCC composite NF membrane had a low-molecular weight cut-off but better permeability and a relatively high level of retention of the $MgCl_2$ solution.

3.4.2. Rejection of PPCPs

The rejection rates of the PEI/TMC/HTCC membrane to CBZ, IBU, ATE and AML were 86.02, 77.21, 89.64 and 90.12% in Figure 6, respectively, which were greater than 75%, proving that the PEI/TMC/HTCC membrane showed great performance in removing PPCPs. The PEI/TMC/HTCC membrane had the highest removal rate of PPCPs with the positive charge (ATE and AML), followed by neutral CBZ, and the lowest removal rate of negatively charged IBU, suggesting the positive charge of the surface of the membrane indirectly (Xu *et al.* 2019b). The surface of the positively charged membrane hindered the penetration of the isoelectric ions by electrostatic repulsion while attracting the ions with the opposite charge to penetrate the

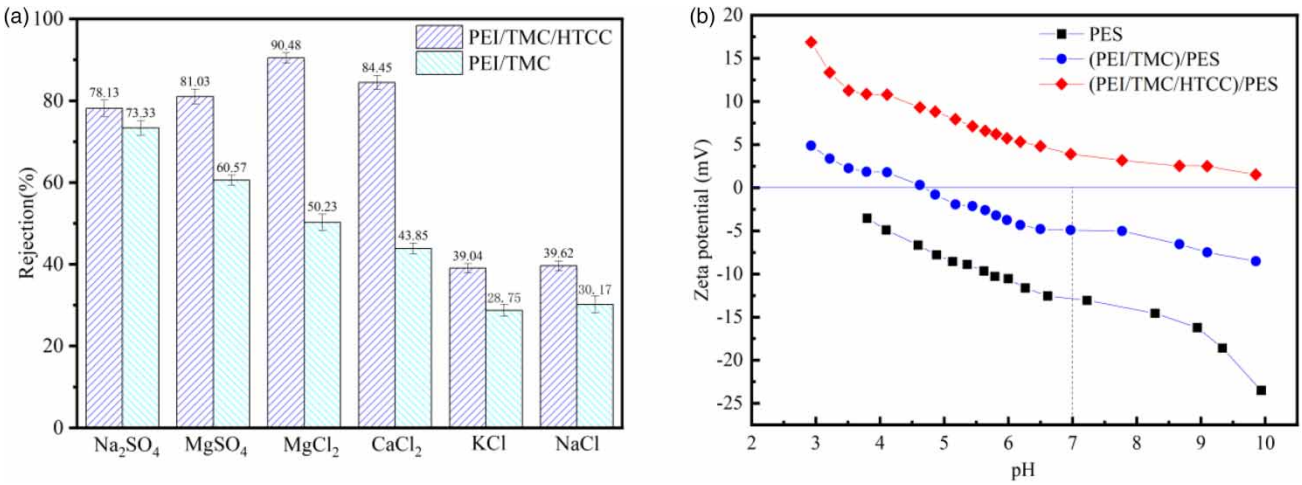

Figure 5 | Retention of different salts (a) and Zeta potential (b) in various pH conditions by the PEI/TMC membrane and the PEI/TMC/HTCC membrane.

Table 1 | Comparison of water permeability and separation properties between the current results and other available NF membranes

Membranes	Pore water pressure ($L \cdot m^{-2} \cdot h^{-1} \cdot Mpa^{-1}$)	Salt rejection (%)		Salt concentration (mg/L)	MWCO (Da)	Ref.
		$MgCl_2$	Na_2SO_4			
PEI/TMC/HTCC	25.37	90.48	78.13	500	481	This work
$(HTCC/PDA)_3$ NF	15.67	47.9	72	500	935	Ouyang *et al.* (2019)
HTCC/PES	20.0	74.5	30.4	500	968	Huang *et al.* (2016)
EDTA-modified NF	6.0	84.6	83.1	2,000	292	Li *et al.* (2017)
NTR-7450	109	16	92	1,000	/	Schaep *et al.* (1998)
Hollow fiber NF	/	70.4	/	1,000	850	Li *et al.* (2015)

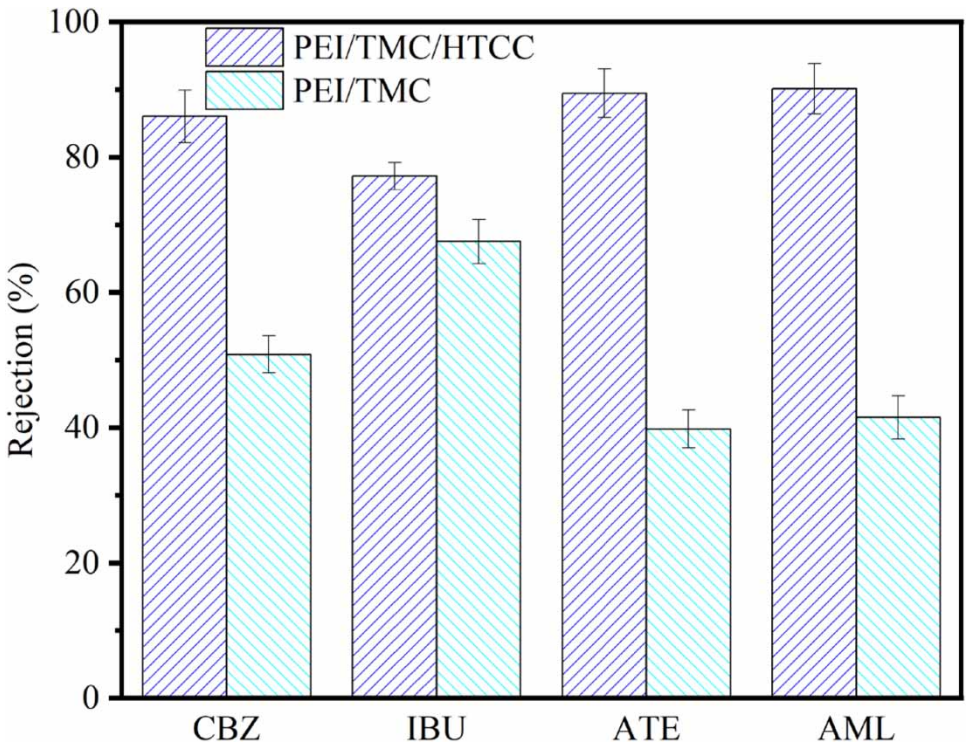

Figure 6 | Rejection of CBZ, IBU, ATE, and AML of the PEI/TMC membrane and the PEI/TMC/HTCC membrane.

surface of the membrane so that the composite membrane had the highest rejection rate of AML and ATE. As shown in Table 2, the relative molecular weight of AML was greater than that of ATE. In addition to the charge effect, the sieving effect also played a certain role (Wang *et al.* 2018). Therefore, the removal rate of AML by the composite membrane was

Table 2 | Physicochemical characteristics of selected PPCPs (n.a.: not applicable)

PPCPs	Molecular weight ($g \cdot mol^{-1}$)	Octanol/water distribution coefficient ($\log K_{ow}$)	Dissociation constant (pK_a)	Charge (pH = 7)	Category
ATE	266.3	0.16	9.43	+	Hydrophilicity
IBU	206.3	3.97	4.47	−	Hydrophobicity
CBZ	236.3	2.45	7.00	Neutral	Hydrophobicity
AML	408.9	n.a.	8.60	+	n.a.

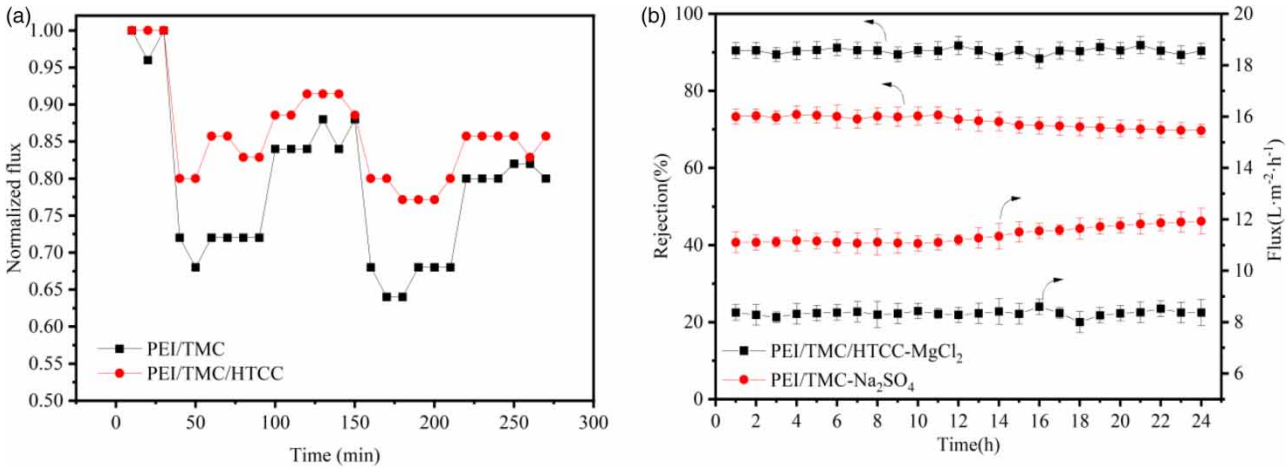

Figure 7 | Anti-fouling performance (a) and stability (b) of the PEI/TMC membrane and the PEI/TMC/HTCC membrane.

greater than ATE, up to 90.12%. On the contrary, the PEI/TMC composite membrane with a loose surface structure possessed a relatively low removal rate of PPCPs, but the interception order still conformed to the interception law of the negatively charged composite NF membrane, namely IBU > CBZ > AML > ATE.

3.5. Anti-fouling performance and stability

As illustrated in Figure 7(a), the flux recovery rate index FRR and flux loss rate index DR_t were calculated through the membrane initial flux J_0, the flux of membrane J_P, and the membrane recovery flux J_t, characterizing the flux recovery rate by formula (4) and formula (5). The higher the FRR value or the lower the DR_t value, the stronger the anti-fouling performance (Fang *et al.* 2012; Liu *et al.* 2018b). The FRR value and the DR_t value of the PEI/TMC/HTCC composite membrane were 0.85 and 0.21, respectively. The FRR value and the DR_t value of the PEI/TMC composite membrane were 0.81 and 0.33, respectively. Compared with the PEI/TMC composite membrane, the PEI/TMC/HTCC composite membrane had stronger anti-fouling performance than the PEI/TMC composite membrane due to the better anti-fouling ability of HTCC and the smoother membrane surface. It can be seen that the rejection and flux of 0.5 g/L $MgCl_2$ and Na_2SO_4 changed with time. The rejection of Na_2SO_4 by the PEI/TMC membrane was stable at about 73%, while the flux was stable at 11.5 $L{\cdot}m^{-2}{\cdot}h^{-1}$. The rejection of $MgCl_2$ by the PEI/TMC/HTCC membrane was stable at about 90%, and the flux was stable at 8.5 $L{\cdot}m^{-2}{\cdot}h^{-1}$. Therefore, after further modification of the PEI/TMC composite membrane by HTCC, the PEI/TMC/HTCC membrane was more stable because of the formation of a more compact surface layer.

4. CONCLUSIONS

We have successfully prepared a positively charged composite NF membrane that has been modified with HTCC containing quaternarized chitosan. It is prepared from natural chitosan for the removal of PPCPs through SIP. The concentration of PEI and its soaking time and the concentration of HTCC and its soaking time were determined as 1.5%, 20 min and 0.5%, 15 min to achieve the optimal membrane, respectively. The surface microstructure of the optimal membrane was studied by SEM and AFM. The amphoteric membrane showed a MWCO of 481 Da. Our experimental results indicated that the PEI/TMC/HTCC membrane exhibited excellent rejection performance to various inorganic salts and PPCPs by Donnan exclusion and steric hindrance. At the same time, the anti-fouling performance and stability of the PEI/TMC/HTCC membrane were improved. Therefore, this study provides a new strategy for the preparation of NF membranes in the removal of PPCPs.

ACKNOWLEDGEMENTS

Our work was financially supported by the National Natural Science Foundation of China (Grant No. 51208259). Facility support was acknowledged to the Jiangsu Key Laboratory of Chemical Pollution Control and Resources Reuse, Nanjing University of Science and Technology (Grant No. 30920140122008).

DATA AVAILABILITY STATEMENT

All relevant data are included in the paper or its Supplementary Information.

CONFLICT OF INTEREST

The authors declare there is no conflict.

REFERENCES

Afonso, M. D., Hagmeyer, G. & Gimbel, R. 2001 Streaming potential measurements to assess the variation of nanofiltration membranes surface charge with the concentration of salt solutions. *Separation & Purification Technology* **22–23** (1–3), 529–541.

Bellona, C. & Drewes, J. E. 2007 Viability of a low-pressure nanofilter in treating recycled water for water reuse applications: A pilot-scale study. *Water Research* **41** (17), 3948–3958.

Bi, R., Zhang, Q., Zhang, R. N., Su, Y. L. & Jiang, Z. Y. 2018 Thin film nanocomposite membranes incorporated with graphene quantum dots for high flux and antifouling property. *Journal of Membrane Science* **553**, 17–24.

Bridge, A. T., Pedretti, B. J., Brennecke, J. F. & Freeman, B. D. 2022 Preparation of defect-free asymmetric gas separation membranes with dihydrolevoglucosenone (Cyrene™) as a greener polar aprotic solvent. *Journal of Membrane Science* **644**, 120173.

Chiao, Y. H., Patra, T., Ang, M. B. M. Y., Chen, S. T., Almodovar, J., Qian, X. H., Wickramasinghe, S. R., Hung, W. S., Huang, S. H., Chang, Y. & Lai, J. Y. 2020 Zwitterion co-polymer PEI-SBMA nanofiltration membrane modified by fast second interfacial polymerization. *Polymers* **12** (2), 269.

Dai, G. H., Huang, J., Chen, W. W., Wang, B., Yu, G. & Deng, S. B. 2014 Major pharmaceuticals and personal care products (PPCPs) in wastewater treatment plant and receiving water in Beijing, China, and associated ecological risks. *Bulletin of Environmental Contamination & Toxicology* **92** (6), 655–661.

El-Gendi, A., Favre, E. & Roizard, D. 2018 Asymmetric polyetherimide membranes (PEI) for nanofiltration treatment. *European Polymer Journal* **105**, 204–216.

Ellis, J. B. 2006 Pharmaceutical and personal care products (PPCPs) in urban receiving waters. *Environmental Pollution* **144** (1), 184–189.

Fang, W. X., Wang, R., Chou, S. R., Setiawan, L. & Fane, A. G. 2012 Composite forward osmosis hollow fiber membranes: Integration of RO- and NF-like selective layers to enhance membrane properties of anti-scaling and anti-internal concentration polarization. *Journal of Membrane Science* **394–395**, 140–150.

Fatta-Kassinos, D., Meric, S. & Nikolaou, A. 2011 Pharmaceutical residues in environmental waters and wastewater: Current state of knowledge and future research. *Analytical & Bioanalytical Chemistry* **399** (1), 251–275.

Gu, Z. Y., Yu, S. L., Zhu, J. Y., Li, P., Gao, X. R. & Zhang, R. J. 2020 Incorporation of lysine-modified UiO-66 for the construction of thin-film nanocomposite nanofiltration membrane with enhanced water flux and salt selectivity. *Desalination* **493**, 114661.

Guo, S. W., Wan, Y. H., Chen, X. R. & Luo, J. Q. 2021 Loose nanofiltration membrane custom-tailored for resource recovery. *Chemical Engineering Journal* **409**, 127376.

Huang, Z. H., Li, W. J., Liu, Z. L. & Zhang, Y. 2015 One pot blending of biopolymer-TiO_2 composite membranes with enhanced mechanical strength. *Journal of Applied Polymer Science* **132** (45), 12951–12959.

Huang, Z. H., Yin, Y. N., Aikebaier, G. L. M. L. & Zhang, Y. 2016 Preparation of a novel positively charged nanofiltration composite membrane incorporated with silver nanoparticles for pharmaceuticals and personal care product rejection and antibacterial properties. *Water Science & Technology* **73** (8), 1910–1919.

Kong, X., Zhou, M. Y., Lin, C. E., Wang, J., Zhao, B., Wei, X. Z. & Zhu, B. K. 2016 Polyamide/PVC based composite hollow fiber nanofiltration membranes: Effect of substrate on properties and performance. *Journal of Membrane Science* **505**, 231–240.

Kosma, C. I., Lambropoulou, D. A. & Albanis, T. A. 2010 Occurrence and removal of PPCPs in municipal and hospital wastewaters in Greece. *Journal of Hazardous Materials* **179** (1), 804–817.

Kosma, C. I., Lambropoulou, D. A. & Albanis, T. A. 2014 Investigation of PPCPs in wastewater treatment plants in Greece: Occurrence, removal and environmental risk assessment. *Science of the Total Environment* **466–467** (1), 421–438.

Košutić, K., Dolar, D., Ašperger, D. & Kunst, B. 2007 Removal of antibiotics from a model wastewater by RO/NF membranes. *Separation & Purification Technology* **53** (3), 244–249.

Lee, H. J., Jung, B., Kang, Y. S. & Lee, H. 2004 Phase separation of polymer casting solution by nonsolvent vapor. *Journal of Membrane Science* **245** (1–2), 103–112.

Li, X. H., Zhang, C. J., Zhang, S. N., Li, J. X., He, B. Q. & Cui, Z. Y. 2015 Preparation and characterization of positively charged polyamide composite nanofiltration hollow fiber membrane for lithium and magnesium separation. *Desalination* **369**, 26–36.

Li, W., Shi, C., Zhou, A. Y., He, X., Sun, Y. W. & Zhang, J. L. 2017 A positively charged composite nanofiltration membrane modified by EDTA for LiCl/$MgCl_2$ separation. *Separation and Purification Technology* **186**, 233–242.

Li, Q. X., Huang, Z. H., Lin, X. L., Zhu, Y. H. & Bai, X. H. 2022 A super-hydrophilic partially reduced graphene oxide membrane with improved stability and antibacterial properties. *Water Science and Technology* **86** (6), 1426–1443.

Lin, Y. L., Tsai, C. C. & Zheng, N. Y. 2018 Improving the organic and biological fouling resistance and removal of pharmaceutical and personal care products through nanofiltration by using in situ radical graft polymerization. *Science of the Total Environment* **635**, 543–550.

Lin, Y. L., Tsai, J. Z. & Hung, C. H. 2019 Using in situ modification to enhance organic fouling resistance and rejection of pharmaceutical and personal care products in a thin-film composite nanofiltration membrane. *Environmental Science and Pollution Research* **26**, 34073–34084.

Liu, Y. L., Wang, X. M., Yang, H. W. & Xie, Y. F. F. 2018a Adsorption of pharmaceuticals onto isolated polyamide active layer of NF/RO membranes. *Chemosphere* **200**, 36–47.

Liu, J. X., Wang, Z. H., Tang, C. Y. Y. & Leckie, J. O. 2018b Modeling dynamics of colloidal fouling of RO/NF membranes with a novel collision-attachment approach. *Environmental Science & Technology* **52** (3), 1471–1478.

Liu, N., Jin, X. W., Feng, C. L., Wang, Z. J., Wu, F. C., Johnson, A. C., Xiao, H. X., Hollert, H. & Giesy, J. P. 2020 Ecological risk assessment of fifty pharmaceuticals and personal care products (PPCPs) in Chinese surface waters: A proposed multiple-level system. *Environment International* **136**, 105454.

Liu, J., Ge, S., Shao, P., Wang, J. F., Liu, Y. J., Wei, W., He, C. & Zhang, L. L. 2023 Occurrence and removal rate of typical pharmaceuticals and personal care products (PPCPs) in an urban wastewater treatment plant in Beijing, China. *Chemosphere* **339**, 139644.

Mansourpanah, Y., Alizadeh, K., Madaeni, S. S., Rahimpour, A. & Soltani Afarani, H. 2011 Using different surfactants for changing the properties of poly(piperazineamide) TFC nanofiltration membranes. *Desalination* **271** (1–3), 169–177.

Montforts, M. H. M. M. 2006 Validation of the exposure assessment for veterinary medicinal products. *Science of the Total Environment* **358** (1–3), 121–136.

Oatley-Radcliffe, D. L., Walters, M., Ainscough, T. J., Williams, P. M., Mohammad, A. W. & Hilal, N. 2017 Nanofiltration membranes and processes: A review of research trends over the past decade. *Journal of Water Process Engineering* **19**, 164–171.

Oluwole, A. O., Omotola, E. O. & Olatunji, O. S. 2020 Pharmaceuticals and personal care products in water and wastewater: A review of treatment processes and use of photocatalyst immobilized on functionalized carbon in AOP degradation. *BMC Chemistry* **14** (62), 1–29.

Ouyang, Z. Y., Huang, Z. H., Tang, X. Y., Xiong, C. H., Tang, M. D. & Lu, Y. T. 2019 A dually charged nanofiltration membrane by pH-responsive polydopamine for pharmaceuticals and personal care products removal. *Separation and Purification Technology* **211**, 90–97.

Radjenović, J., Petrović, M., Ventura, F. & Barceló, D. 2008 Rejection of pharmaceuticals in nanofiltration and reverse osmosis membrane drinking water treatment. *Water Research* **42** (14), 3601–3610.

Schaep, J., Bruggen, B. V. D., Vandecasteele, C. & Wilms, D. 1998 Influence of ion size and charge in nanofiltration. *Separation & Purification Technology* **14** (1–3), 155–162.

Semião, A. J. C. & Schäfer, A. I. 2013 Removal of adsorbing estrogenic micropollutants by nanofiltration membranes: Part A – Experimental evidence. *Journal of Membrane Science* **431**, 244–256.

Semião, A. J. C., Foucher, M. & Schäfer, A. I. 2013 Removal of adsorbing estrogenic micropollutants by nanofiltration membranes: Part B – Modeldevelopment. *Journal of Membrane Science* **431**, 257–266.

Shen, K., Cheng, C., Zhang, T. H. & Wang, X. F. 2019 High performance polyamide composite nanofiltration membranes via reverse interfacial polymerization with the synergistic interaction of gelatin interlayer and trimesoyl chloride. *Journal of Membrane Science* **588**, 117–192.

Shen, Q., Xu, S. J., Dong, Z. Q., Zhang, H. Z., Xu, Z. L. & Tang, C. Y. Y. 2020 Polyethyleneimine modified carbohydrate doped thin film composite nanofiltration membrane for purification of drinking water. *Journal of Membrane Science* **610**, 118220.

Tang, B. B., Huo, Z. B. & Wu, P. Y. 2008 Study on a novel polyester composite nanofiltration membrane by interfacial polymerization of triethanolamine (TEOA) and trimesoyl chloride (TMC) I. Preparation, characterization and nanofiltration properties test of membrane. *Journal of Membrane Science* **320** (1–2), 198–205.

Tao, L., Wang, X. J., Wu, F. D., Wang, B. H., Gao, C. J. & Gao, X. L. 2022 Highly efficient Li^+/Mg^{2+} separation of monovalent cation permselective membrane enhanced by 2D metal organic framework nanosheets. *Separation and Purification Technology* **296**, 121309.

Tsuru, T., Sasaki, S., Kamada, T., Shintani, T., Ohara, T., Nagasawa, H., Nishida, K., Kanezashi, M. & Yoshioka, T. 2013 Multilayered polyamide membranes by spray-assisted 2-step interfacial polymerization for increased performance of trimesoyl chloride (TMC)/m-phenylenediamine (MPD)-derived polyamide membranes. *Journal of Membrane Science* **446** (11), 504–512.

Wang, D. L., Li, K. & Teo, W. K. 2002 Preparation of asymmetric polyetherimide hollow fibre membrane with high gas selectivities. *Journal of Membrane Science* **208** (1), 419–426.

Wang, Y. G., Wang, X., Li, M. W., Dong, J., Sun, C. H. & Chen, G. Y. 2018 Removal of pharmaceutical and personal care products (PPCPs) from municipal waste water with integrated membrane systems, MBR-RO/NF. *International Journal of Environmental Research & Public Health* **15** (2), 269.

Xiang, J., Li, H., Hei, Y. H., Tian, G. Y., Zhang, L., Cheng, P. G., Zhang, J. P. & Tang, N. 2022 Preparation of highly permeable electropositive nanofiltration membranes using quaternized polyethyleneimine for dye wastewater treatment. *Journal of Water Process Engineering* **48**, 102831.

Xu, J., Wang, Z., Wang, J. X. & Wang, S. C. 2015 Positively charged aromatic polyamide reverse osmosis membrane with high anti-fouling property prepared by polyethylenimine grafting. *Desalination* **365**, 398–406.

Xu, P., Wang, W., Qian, X. M., Wang, H. B., Guo, C. S., Li, N., Xu, Z. W., Teng, K. Y. & Wang, Z. 2019a Positive charged PEI-TMC composite nanofiltration membrane for separation of Li^+ and Mg^{2+} from brine with high Mg^{2+}/Li^+ ratio. *Desalination* **449**, 57–68.

Xu, R., Zhang, P., Wang, Q., Wang, X. M., Yu, K. C., Xue, T. & Wen, X. H. 2019b Influences of multi influent matrices on the retention of PPCPs by nanofiltration membranes. *Separation and Purification Technology* **212**, 299–306.

Zhang, X. Y., Chan-Yu-King, R., Jose, A. & Manohar, S. K. 2004 Nanofibers of polyaniline synthesized by interfacial polymerization. *Synthetic Metals* **145** (1), 0–29.

Zhang, R. N., Su, Y. L., Zhao, X. T., Li, Y. F., Zhao, J. J. & Jiang, Z. Y. 2014 A novel positively charged composite nanofiltration membrane prepared by bio-inspired adhesion of polydopamine and surface grafting of poly(ethylene imine). *Journal of Membrane Science* **470**, 9–17.

Zhang, R. N., Su, Y. L., Zhou, L. J., Zhou, T. T., Zhao, X. T., Li, Y. F., Liu, Y. N. & Jiang, Z. Y. 2016 Manipulating the multifunctionalities of polydopamine to prepare high-flux anti-biofouling composite nanofiltration membranes. *RSC Advances* **6**, 32863–32873.

Zhao, Y. Y., Kong, F. X., Wang, Z., Yang, H. W., Wang, X. M., Xie, Y. F. F. & Waite, T. D. 2017 Role of membrane and compound properties in affecting the rejection of pharmaceuticals by different RO/NF membranes. *Frontiers of Environmental Science & Engineering* **11** (6), 183–195.

First received 3 December 2023; accepted in revised form 20 March 2024. Available online 9 April 2024